

"Made available under NASA sponsorship  
in the interest of early and wide dis-  
semination of Earth Resources Survey  
Program information and without liability  
for any use made thereof."

E7.6-10306

NASA CR-  
147548

FINAL REPORT

S-149 Micrometeorite Collection Experiment

Contract NAS9-10380

Submitted to: Johnson Space Flight Center  
Houston, Texas

Submitted by:

*Curtis L. Hemenway*

Curtis L. Hemenway  
Principal Investigator

(E76-10306) S-149 MICROMETEORITE COLLECTION N76-22625  
EXPERIMENT Final Report (Dudley  
Observatory) 50 p HC \$4.00 CSCI 03B  
Unclas  
G3/43 00306

Dudley Observatory  
100 Fuller Road  
Albany, New York 12205

## INTRODUCTION

The S-149 experiment was an outgrowth of the S-18 experiment which was designed for use in the Apollo program. Both programs were follow-on experiments based on the experience gained from the S-10 and S-12 experiments from Gemini.

The experiment was conceived, designed, developed and fabricated at Dudley Observatory and most of the data analysis is currently being carried out at Dudley Observatory. The hardware consisted of four sets of sample carrying cassettes which were to be deployed by a motor driven device. A full description of the engineering operation has been given in a previous report and is included as Appendix A.

The actual scientific experiment was intended to provide scientific information in four general areas:

1. A measurement of the cosmic dust flux in near-earth space over the mass range  $10^{-5}$  to  $10^{-7}$  grams.
2. A search for anisotropy in the directional distribution of cosmic dust particles.
3. A measurement of the chemical composition of cosmic dust as determined by residues of the particles remaining on the interior of the crater walls.
4. Evidence of particle structural strength.

A variety of highly polished solid surfaces, thin metal foils, and thin plastic films (see Appendix B for a description of the individual sample types and their distribution within the cassettes) were prepared to record the impact events and provide the desired data. Since at the limit of resolution of an optical system, impact structures can become confused with artifacts, a very considerable effort was devoted to controlling any background structure which might be confused with a real impact event. When one examines surfaces at high magnification this is far from a trivial problem.

The original flight plan called for four exposures of 3 days, 30 days, 10 days and 30-60 days. After the launch and subsequent loss of the use of the solar airlock the extraordinary efforts of the staff at JSC aided by Dudley personnel enabled us to obtain exposures of 46 and 33 days in the solar facing direction which was far more than we would have hoped for under the circumstances. These two exposures together with a 34 day exposure through the anti-solar airlock have already provided a large body of data concerning cosmic dust in the vicinity of the earth. A fourth set of samples was deployed before the astronauts left Skylab to be recovered on some possible future mission to Skylab.

Appendix C is a summary of the first results of the analysis of the S-149 samples presented at the AIAA/AGU Conference on Scientific Experiments of Skylab in Huntsville. Appendix D is a preprint of a

paper presented at COSPAR in Varna, Bulgaria on the gold foil experiments and Appendix E is a preprint of a paper on the crater studies given at IAU Colloquium 31 in Heidelberg, Germany.

The following summarizes results obtain under this contract and indicates some further work to be done.

### CRATER STUDIES

Light optical scanning has been the prime method for the detection of impact craters on the various surfaces. With all of the surfaces scanned at 200X magnification and about 25% re-examined at 500X a total of 54 craters have been found ranging from 2 micron diameter to 135 micron diameter. In addition four sub-micron craters have been found after scanning  $30\text{mm}^2$  in the scanning electron microscope. The fluxes determined from this data are shown in Figure 1. There is only a small difference between the solar and the anti solar fluxes but a somewhat larger difference exists between the fluxes which correspond to covers and pans. The four sub-micron craters are represented by the two points between  $10^{-15}$  and  $10^{-14}$  grams, indicating a very sharp three orders of magnitude discontinuity in the flux curve. The spacecraft was highly stabilized along the Z axis but was allowed to oscillate about that axis with the resulting effect that the pans sensed particles in nearly circular orbits in the plane of the earth's orbit. On the other hand the covers were sensitive to particles in

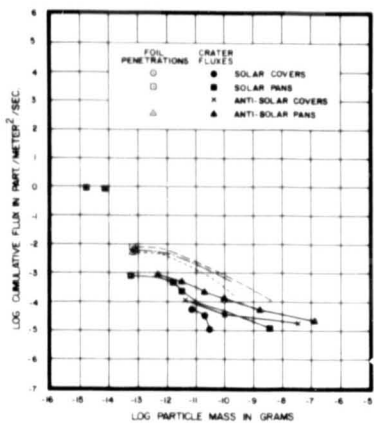


Figure 1.

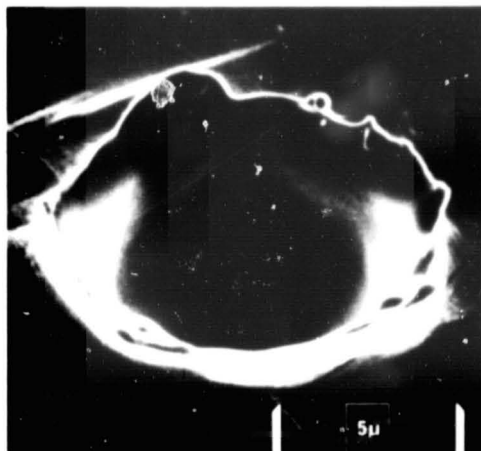


Figure 2.

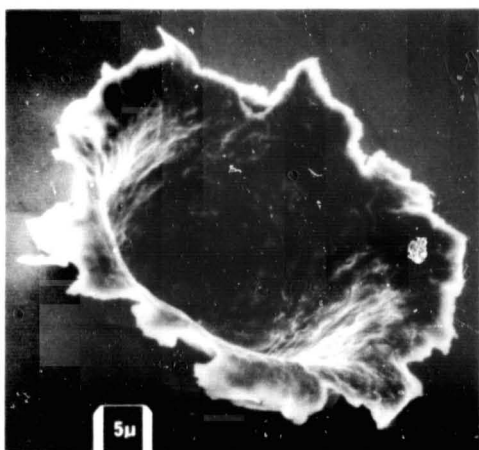


Figure 3.

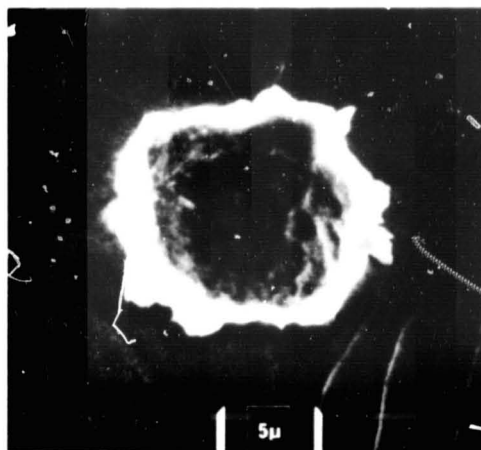


Figure 4.

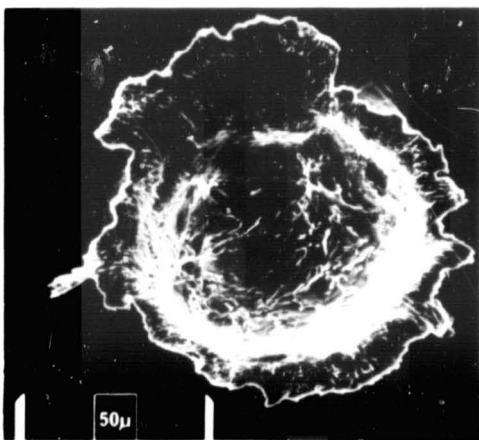


Figure 5.

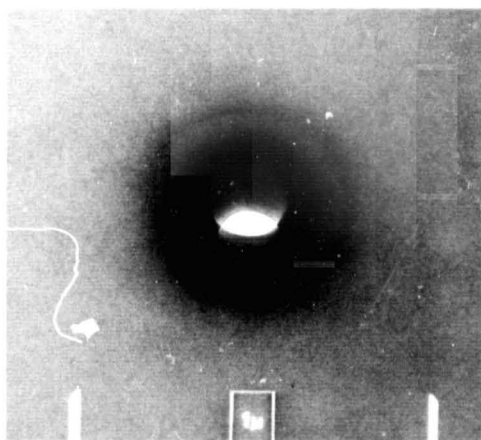


Figure 6.



highly eccentric orbits or moving radially outward from the solar direction. The relative scarcity of crater impact events on the covers indicates that the crater forming particles are predominately in nearly circular orbits.

Significant meteor showers, the Perseids and the Geminids, occurred during two of the exposures and would have been detected had there been a large population of small meteoroids in the meteor stream. The lack of enhancement indicates that particles smaller than about  $10^{-8}$  grams are not present in large numbers in these streams.

Figures 2-5 illustrate some typical craters and show variations in the morphology of the interior. All but two craters greater than one micron diameter are round. In addition to classic craters fourteen sub-micron non-circular structures have been observed in the scanning electron microscope. Some of these were produced by grazing impact but the mechanism for the formation of the remaining structure has not yet been determined. Many of these irregular structures are similar to structures found on samples exposed on the Gemini S-10 experiment. Non-circular impacts have been produced in test firings by particles directed more than  $45^{\circ}$  from the normal to the surface. These results were obtained in firings at both Goddard Space Flight Center and the Max-Planck-Institut at Heidelberg, Germany.

Table I lists the dimensions of the craters and their diameter to depth ratios. In addition, on all of the craters greater than 15

FOLDOUT FRAME 2

	Solar SL/3		Solar SL/4		Anti-Solar SL 2/3	
	DIA (micron)	DIA/Depth	DIA (micron)	DIA/Depth	DIA (micron)	DIA/Depth
<b>Cassette</b>						
<b>A-Pan</b>	1.5	-	3.4	3.4	7.8	3.0
	1.5	-			10.4	2.5
	2.0	-			19.5	2.0
	2.0	2.2			20.8	1.8
	2.0	2.5			31.2	2.0
	2.2	2.2			135.2	2.0
	2.5	-				
	2.6	-				
	2.6	-				
	2.6	-				
	2.7	-				
	4.0	-				
	5.8	2.3				
	5.8	1.9				
	6.5	3.3				
	7.8	3.1				
	15.0	-				
<b>A-Cover</b>	-	-	-	-	4.5	4.5
	-	-	-	-	86.0	2.2
<b>B-Pan</b>	2.2	2.8	1.8	-	3.8	2.5
	5.2	1.3			3.9	1.8
	6.5	2.2			6.9	2.5
	7.8	2.8			11.7	2.8
	15.0	2.9				
<b>B-Cover</b>	46.8	2.1	-	-	6.0	3.0
<b>C-Pan</b>	3.9	2.2	1.3	-	2.1	-
	3.9	2.8	1.8	-	2.3	-
	4.5	2.3	2.5	-	4.9	4.1
			2.5	2.5	5.2	3.2
			2.6	-	5.4	3.0
			2.6	2.6	5.4	3.6
			2.6	2.5	5.6	3.1
			3.7	3.7	6.5	3.0
			3.9	3.9	6.5	3.2
			4.5			

	5.8	1.9				
	6.5	3.3				
	7.8	3.1				
	15.0	-				
A-Cover	-	-	-	-	4.5	4.5
	-	-	-	-	86.0	2.2
B-Pan	2.2	2.8	1.8	-	3.8	2.5
	5.2	1.3			3.9	1.8
	6.5	2.2			6.9	2.5
	7.8	2.8			11.7	2.8
	15.0	2.9				
B-Cover	46.8	2.1		-	6.0	3.0
C-Pan	3.9	2.2	1.3	-	2.1	-
	3.9	2.8	1.8	-	2.3	-
	4.5	2.3	2.5	-	4.9	4.1
			2.5	2.5	5.2	3.2
			2.6	-	5.4	3.0
			2.6	2.6	5.4	3.6
			2.6	2.5	5.6	3.1
			3.7	3.7	6.5	3.0
			3.9	3.9	6.5	3.2
			4.5			
			4.6	3.2		
			5.2	5.2		
			6.5	3.3		
C-Cover	-	-	7.8	5.2	5.2	5.2
			8.0	2.7		
D-Pan	4.0	4.0	1.3	-	4.0	2.7
	4.3	2.9	2.5	-	12.6	3.2
	18.2	1.9	20.8	2.3		
D-Cover	5.8	1.9	6.5	3.3	6.5	2.4
					14.3	2.3
Exposure Duration	46 days		33 days		34 days	

Table I  
Crater Sizes and Distribution

NO. 1000000



micron diameter the contour of the crater interior has been measured which showed the craters to have essentially hemispherical or conical shapes.

The interiors of about half of the craters have been examined using energy dispersive X-ray emission analysis to try to detect remnants of the impacting particle. While it is not possible to determine the specific identity of the impacting particle, significant residues were detected. It is interesting to note that the ability to detect residues is independent of crater size. The next to the largest crater (86 micron diameter) produced no detectable X-ray emission while other craters as small as 2 microns have revealed detectable residues. Table II lists the craters studied and the elements detected. The most surprising point is the high incidence of craters with aluminum residues. Secondary impacts can be discounted as a possibility for most of these because they occur on the anti-solar facing samples as well as on the solar facing samples where the unit was located close to the dish of the Apollo Telescope Mount. Considering the small area of collector exposed as compared to the sample surface the observed flux would have to be very high for secondaries to have contributed measurably to the observed number of craters. A possible source for some of the craters could be from particles ejected from other spacecraft, which have become space contaminants.

All attempts to draw correlations among the various observations

Type	Dia ( $\mu$ )	Dia/depth	Elements						
<u>Smooth</u>									
B-1-12-2	5.2	4.3	Al						
C-2-9-9-2	1.8					Cr	Fe	Ni	
<u>Melted</u>									
B-1-12-1	47	2.1					Fe		
A-3-15-2	21	1.8	Al						
A-3-16-2	20	1.9	Al						
A-3-16-3	31	1.9	Al						
<u>Lumpy</u>									
B-1-12-4	15	3.9	Mg	Al	Si	S	K	Fe	Ca
B-2-9-3-1	1.8	-			Si	S	Zn		
B-3-15-9-1	12	2.6		Al					
<u>Textured</u>									
B-1-12-3	7.8	2.8	Mg		Si				
D-2-16-8-1	2.5	-		Al	Si				
A-3-15-1	7.8	3.0		Al					
B-3-13-1	6.9	2.5			Si	S		Fe	
C-3-14-1	5.6	3.1		Al					
C-3-14-2	5.4	3.6		Al					
C-3-14-4	4.9	4.1		Al					
C-3-14-5	6.5	3.3		Al					
C-3-16-1	2.1	-		Al	Si				

Table II

Residues Detected within Craters

on the structure, chemistry or distribution of the craters indicate that as yet we do not know enough about the details of crater formation to be able to relate all of the observed data.

In studying the distribution of events it is apparent that some clustering of events is being observed. On three pan slides the number of events is five times the overall average for pan slides.

### GOLD FOILS

A detailed discussion of the results of the gold foil experiment is given in Appendix D; therefore, only a summary of the conclusions is given here.

This experiment has shown that there exists a population of cosmic dust particles which is more numerous than those producing impact craters by about a factor of ten. See Figure 1 for the fluxes. Not only are these particles more numerous but they are clearly of a very different physical structure as evidenced by the observed break-up the particles experience when they penetrate a gold foil. Their extreme fragility was demonstrated by the case of one particle which was shown to have approached within 1-2 cm of the gold foil before it shattered into about 5000 pieces.

Clustering has also been detected by the gold foils. Pairs of holes a few microns apart and groups of holes have been observed.

On one of the solar exposures secondary events originating from

the dish of the Apollo Telescope Mount were detected.

Chemical analysis of residues associated with penetration holes has had limited success because of the extremely small quantities of material present.

### EVIL EYES

In the Gemini S-12 experiment a strange structure was observed on thin nitrocellulose films. It was clear that they had been added in flight but very little more could be said of them. This structure was again observed on the S-149 experiment. It appears that the particles producing the "evil eye" must be of two components; a core which has sufficient mass to penetrate the film and a coating which is left behind on the nitrocellulose films as shown in Figure 6.

### CORROSION

Among the samples exposed were, as mentioned, highly polished silver and copper plates. On the solar facing exposures the samples nearest to the Apollo Telescope Mount became corroded to the extent that the oxide layer in some areas peeled away from the surface.

Another sample which suffered damage was a set of thin carbon coated nitrocellulose films which were exposed through the anti-solar airlock. These films completely disappeared. What makes this even more strange is the fact that identical films exposed among solar facing samples survived.

## SUMMARY

Although considerable data has been obtained under this contract a potentially even larger body of data awaits the results of further study. In each of the areas investigated there have been observations whose interpretation has been left unanswered.

Some obvious items are:

1. The reason for the discontinuity in the flux curve at about  $10^{-13}$  grams.
2. The nature of the particles producing the holes in the gold foils.
3. The source of the particles producing the "evil eye" structures.
4. An analysis of the original particles as inferred from residues found in impact craters.

In addition to the above items there were the oxidation effects which occurred on polished copper and silver slides which deserve study.

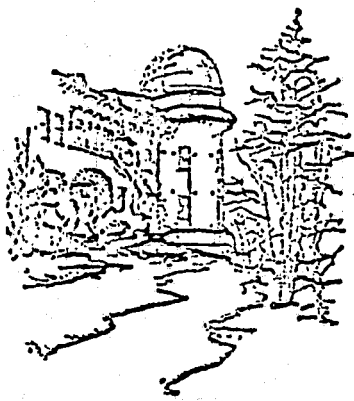
## ACKNOWLEDGEMENTS

We wish to acknowledge the help given during this experiment by the entire staff at JSC in particular the efforts of our technical monitor, Mitchell Wilcox whose extraordinary efforts made it possible for this experiment to exceed its goals even with the loss of the use of the solar airlock. The astronauts not only carried out the experiment deployment with competence and enthusiasm but were extremely helpful in solving the many problems which arose when the solar airlock had to be used to deploy a sunshield to replace the lost meteoroid shield.

We wish to particularly note the support of Mr. Kenneth Kleinknecht and Mr. William Schneider who despite the extraordinary demands on their time always seemed to be available when needed.

We also wish to express our appreciation to Mr. Gustave Bellisari of ONR for his assistance and help in certifying and qualifying the S-149 experiment for flight. His help went far beyond the normal requirements of his job.

The experiment would not have been possible without the dedicated efforts of many people at Dudley, in particular: Donald Tackett, Laurence Bourdillon, Lawrence Brennan, Charles Jones, Barbara Reynolds, John Tarnawski, Anthony Laudate, William Radigan, Richard Schwarz and Douglas Hallgren.



THE DUDLEY OBSERVATORY

(CHARTERED 1852)

100 FULLER ROAD  
ALBANY, NEW YORK

12205

TELEPHONE  
1.518.459.4750

DIRECTOR  
CURTIS HEMENWAY, PH.D.

6 March 1974

APPENDIX A

Mr. Tony C. Riggan  
Code: BC 24  
NASA/Johnson Space Center  
Houston, Texas 77058

Subject: Contract NAS 9-10380 - Final Report on the Hardware Phase of the Contract.

Dear Mr. Riggan:

As the final Skylab Mission has ended I would like to take this opportunity to clean up our technical efforts on the S-149 Contract. As everyone knows the scientific data so far indicates a very successful experiment.

The Contract NAS 9-10380 is divided up into two sections Exhibit A and Exhibit B. I will start by reviewing Exhibit A first. The effort under Exhibit A, the initial phase of the contract was during the period Sept. 2, 1969 to July 2, 1970 which included an extension granted under Supplemental Agreement (S/A #1S). Although the history of the experiment predates this time span the final request for this contract was documented by the letter (Hemenway to Thompson) Sept. 3, 1969.

Working under the requirements contained in Exhibit A the necessary support was provided to establish specifications for, S/A 2S-Exhibit B, the hardware and associated support effort.

The transition from study to hardware contract was reviewed in the letter (Hemenway to McAllum) April 7, 1970. The contractual effort was agreed to during the MSC (JSC)/Dudley fact finding meeting, May 22, 1970. As a result of this meeting and the documents prepared all items from Exhibit A were completed. From this I have concluded that the effort under Exhibit A was accomplished satisfactorily.

The major effort to date of this contract was accomplished under S/A 2S Exhibit B, and Supplemental Agreements up to and including 30C and the supporting Contract Change Authorizations CCA's 1 - 45 inclusive.

I will go through each of the items in Exhibit B and then summarize my understanding as to where the contract effort stands to date.



Paragraph 1.0 - 2.0 - Introduction and Scope

The Introduction and Scope are general in nature and the only change was to update the End Item Specification (EIS) as a result of S/A #4.

Paragraph 3.0 - General Requirements

Task 1 - Design Definition

The equipment design was reviewed through the procedures required by the EIS that is; PDR, CDR, CARR and finally the Flight Worthiness Review at KSC, and the final certification documented by JSC letter NB/73-L 213 dated July 26, 1973. There were no constraints or open items on the flight hardware as flown. The launch configuration was documented by Specification Change Notices (SCN's) 1 - 91 inclusive.

Task 2 - Documentation

- A. All documentation required to support the (as launched) hardware effort under the EIS has been completed satisfactorily and no open items remain.
- B. The monthly status report will continue to the contract's conclusion.
- C. Hardware photo documentation has been completed leaving only the effort required to support the scientific data reduction.
- D. The System Safety Plan was approved as part of the General Management Plan DO-GMP-0149.

Task 3 - Interface Control Document

The ICD's were included as part of the work statement including S/A's 14, 19 and 21. This completes the configuration as flown.

Task 4 - Qual Test Hardware

The Qual Test Hardware was delivered under DD 250 S-149-40 dated April 12, 1973 and remains at Dudley Observatory.

**Task 5 - Verification Requirements**

The Verification Requirements were closed with the final verification accomplished by approval of the Qual Test Report, the closing of the Design Certification Review (DCR) action items and the JSC letter NB/73-L 213 dated July 26, 1973.

**Task 6 - Backup Hardware**

The Backup Hardware as defined on the S/A #21 identifies the unit S/N 02 and associated hardware as backup hardware, however S/N 03 and associated hardware was established by Mailgram ED2-73-162 dated February 9, 1973 as backup hardware and was accepted by DD 250 S-149-37 dated April 12, 1973 to remain at Dudley Observatory in controlled storage.

**Task 7 - Flight Hardware**

The Flight Hardware was also incorrect. S/N 02 was delivered as Flight Hardware and successfully flown. The hardware was delivered under DD 250 S-149-4B dated February 14, 1972 and DD 250 S-149-31, dated March 18, 1973, which provided the scientific slides.

**Task 8 - Mockup Hardware**

The unit under this requirement was fabricated and used as described in the letter (Tackett to McCallum) dated September 10, 1970. It is noted in the letter that the hardware was used for the experiment integration studies and crew station review. Because we have no formal buy-off of these items I am enclosing DD 250 - S-149-42 dated March 6, 1974 for signature so that this item can be closed.

**Task 8A - Experiment Training Hardware**

The ETH Mockup was delivered on April 17, 1972 documented by DD 250 S-149-6A.

**Task 9 - Flight Training Type Hardware**

The Engineering Unit was delivered under the direction of telegram ED4 272-8-41 dated August 30, 1972 and shipped to JSC on September 1, 1972 on Dudley Shipper S-149-7. It was brought back

**Task 9 - Continued**

for updating and reshipped on October 20, 1972 on Dudley shipper S-149-12. The unit was modified again and shipped back on January 17, 1973 on Dudley shipper S-149-22. Requests for changes were incorporated according to JSC instructions. This effort was closed out with DD 250 S-149-41 dated January 14, 1974. It should be noted that Task 9 of Paragraph 3.0 as modified by S/A #5 does not agree with the deliverable items as defined by Paragraph 6.0 as modified by S/A #29. I have taken the latter agreement (S/A #29) as being correct.

**Task 10 - The Ground Support and Associated Equipment**

The Ground Support and Associated Equipment have been defined by the initial contract changes and were accepted by their delivery on DD 250 S-149-4C dated February 4, 1972 and DD 250 - S-149-39 dated April 17, 1973. Only CVU S/N 01 and associated hardware remains at Dudley, as requested by JSC.

**Task 11 - Pre-delivery Support**

All necessary pre-delivery support has been successfully accomplished.

**Task 12 - Corrective Action**

The mission objectives have been accomplished therefore I consider this item satisfactorily closed.

**Task 13 - Spares**

The Spare List has been prepared but has not yet been bought-off by JSC. I am enclosing DD 250-43 dated March 6, 1974 for signature so that this item can be closed.

**Task 14 - Module Factory Integration Tests Support**

This item was satisfactorily completed at McDonnell Douglas.

**Task 15 - KSC Support**

This item was satisfactorily accomplished with the completion of the effort at KSC and the launch of SL-1.

Task 16 - Mission Support

This remains open until the completion of the post SL-4 clean up work.

Task 17 - Simulation

All required simulations were successfully accomplished and have been demonstrated by the successful operation of the experiment during the various missions.

Task 18 - Non-conformance Reporting

This effort has been completed with the successful delivery and operation of the experiment.

Task 19 - Parts and Materials Problems

This effort has been completed with the successful delivery and operation of the experiment.

Task 20 - Manned Spacecraft Criteria and Standards

This was completed with the satisfactory delivery of the experiment hardware.

Task 21 - Post Flight Analysis

This will be the major effort until the conclusion of the contract.

Paragraph 4.0 - Management Plan Requirements

The effort under the management plan required by the EIS has been completed with the delivery of the hardware. The necessary contractual management will continue as required to support those items which are to be completed.

Paragraph 5.0 - Program Control Requirements

5.1 - Meetings and Informal Conferences and reviews for the EIS have been completed. However, other meetings and reviews necessary to support the successful scientific analysis will continue.

Paragraph 6.0 - As the items and dates presently documented in this contract are not consistent with the actual delivery dates that were accomplished, I would like to establish that as a result of the various instructions by JSC and those changes and delays accorded Dudley Observatory neither effected the success of the mission or the operation of the experiment. Therefore, I would like to consider the delivery of the hardware completed to our mutual satisfaction.

The plant clearance inventory (non-flight) was turned over to the Dudley Observatory property officer in December for final processing with ONR. It is our intent to request that the residual inventory remain at Dudley to support our other NASA efforts.

I have reviewed our efforts, to date, under the Property Rights and Inventions Clause of the contract and have found none of those efforts applicable.

It is our desire to maintain possession of the existing flight and support hardware because our scientific effort is involved with;

1. The possible recovery of our exposed samples on Skylab from post SL-4 missions.
2. Our desire to support future missions including shuttle, with the present hardware.
3. The studying of artifacts collected on our present samples, should any be found.

The hardware can, if JSC desires, remain in controlled storage here at Dudley as long as required.

In summary, I believe that I have covered all items that are included in the hardware phase of this contract and have provided the necessary justification for my conclusions. Because of the resulting scientific returns I consider the hardware effort completed successfully. I would like to take this opportunity to say that although supporting this effort was very trying on us from time to time, it was gratifying when the goals that were set down so many years ago were realized and with so much success.

Mr. Tony C. Riggan

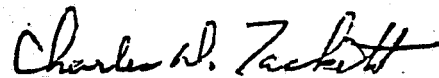
-7-

6 March 1974

There were so many people who helped us with the engineering that it would be impossible to thank them all personally, however, we have not forgotten them and appreciated their help. I can only say, for all of us, that it would be a pleasure to work with them again.

I hope that this letter has cleared up all the loose ends and would appreciate your response as soon as practical.

Sincerely yours,



Charles D. Tackett  
Project Manager/S-149  
NAS 9-10380

CDT/gp

cc: W. Fostel  
G. Bellisari  
J. Wheeler

## APPENDIX B

### Description of Impact Surfaces

#### Polished Plates

Slides 19.4 cm<sup>2</sup> of pure copper, 204L stainless steel and pure silver were polished using metallographic techniques. Care was taken to minimize relief by using nap free polishing until the final clean-up with 0.05 micron alumina. The resulting slides had a surface which had no raised structures which could be confused with impact events. Each slide was prescanned at 100X to note the location of unusual surface imperfections. A random sample of slides was prescanned at 200X to have a record of structures smaller than those seen during the 100X scan. The resulting slides were considered sufficient to seek impact events as small as 1-2 microns by light optical means.

Smaller samples approximately 1 cm<sup>2</sup> were prepared in much the same way for examination in a scanning electron microscope. These samples were shown to be capable of recording events as small as 0.1 - 0.2 microns.

#### Gold Foils

Pure gold foils 500-800 Å thick formed by vapor deposition and supported on 90 mesh copper screening were prepared as another means



to detect particles, principally smaller than 5 microns. The foils were used in single and double layers with a polished stainless steel plate beneath to catch the residues of particles penetrating the foils.

It was anticipated that a measure of directionality could be obtained by aligning the holes or impacts in the foils and stainless steel plates. In order to record the condition of the foils before flight each foil was used as a negative and an image was recorded on photographic paper. All pinholes greater than about three microns were visible to the naked eye on the prints. Subsequently it was shown that in most cases holes as small as one micron could be detected by examining the print using a 7X hand lens.

#### Nitrocellulose Films

In order to detect ultra-small impact events thin (i.e.  $< 500\text{\AA}$ ) carbon coated nitrocellulose films on electron microscope grids were prepared. The grids were mounted on glass cover slips in such a way that the grid position was unambiguously recorded on the cover slip. The intent was to examine the grids in a transmission electron microscope particularly to seek events much smaller than one micron even to events smaller than 0.1 micron. This was to be followed by examination of the glass cover slip in a scanning microscope to locate remnants of the particle which penetrated the thin film.

A second nitrocellulose film experiment was prepared using stacks of three aligned grids. There were two purposes for these grids; first, a small number of pinholes is almost always present in very thin films and it was felt that by being able to see colinear holes uncertainty about the validity of the event would be removed, and secondly the alignment of the holes could be used to provide some directional information.

In order to record the overall effect of space exposure each cassette half was photographed after the samples were loaded and immediately upon return to the laboratory.

#### Guest Experiments

Max-Planck-Institut - Dr. Hugo Fechtig of the Max-Planck-Institut, Heidelberg, Germany provided samples of polished stainless steel, polished mineral sections, and thin metal foils.

Ernest F. Fullam, Inc. - Mr. Ernest F. Fullam of Ernest F. Fullam, Inc., provided thin nitrocellulose films, gold leaf layers, and lexan films. The lexan film was intended to record tracks made by radioactive material.

American Geophysical Union (AGU)  
American Institute of Aeronautics and Astronautics (AIAA)

# AIAA Paper No. 74-1226

APPENDIX C

DUDLEY OBSERVATORY  
REPRINT  
8 49

NEAR-EARTH COSMIC DUST RESULTS FROM S-149

by  
C. L. HEMENWAY  
Dudley Observatory and the State University  
of New York at Albany  
Albany, New York

D. S. HALLGREN AND C. D. TACKETT  
Dudley Observatory  
Albany, New York

## **AIAA/AGU Conference on Scientific Experiments of Skylab**

HUNTSVILLE, ALABAMA/OCT. 30-NOV. 1, 1974

For permission to copy or republish, contact the American Institute of Aeronautics and Astronautics,  
1290 Avenue of the Americas, New York, N.Y. 10019.

ORIGINAL PAGE IS  
OF POOR QUALITY

NEAR-EARTH COSMIC DUST RESULTS FROM S-149

C. L. Hemenway\*  
Dudley Observatory and the State University  
of New York at Albany  
Albany, New York

D. S. Hallgren and C. D. Tackett  
Dudley Observatory  
Albany, New York

Abstract

Three space exposures (34, 46 and 33 days) of thin films and polished metal plates with a total area of  $0.12\text{m}^2$  per exposure were carried out during SKYLAB via the S-149 experiment. Study of the materials recovered indicates that the S-149 experiment contains important information concerning cosmic dust in the near-earth vicinity. Craters and penetration holes have been found ranging from 135 micron diameter to less than 0.5 micron. A cosmic dust flux curve in the mass range from  $10^{-16}$  -  $10^{-7}$  grams is presented. Evidence is given concerning the directional characteristics of the particles and their breakup in near-earth space is presented.

I. Description

The S-149 Experiment consists of the instrument shown in Figure 1, designed to accept a set of four cassettes containing various experimental surfaces and foils to study micrometeorite impacts and penetrations in near-earth space. The instrument allows the unlocking, unsealing and deployment of these cassettes through a scientific airlock, opening of the cassettes by remote control to carry out long duration exposures, closure, retrieval and resealing of the cassettes after each exposure. Figure 2 shows a picture of the S-149 equipment as it would be deployed for exposure, with blank slides in the sample pans and covers.

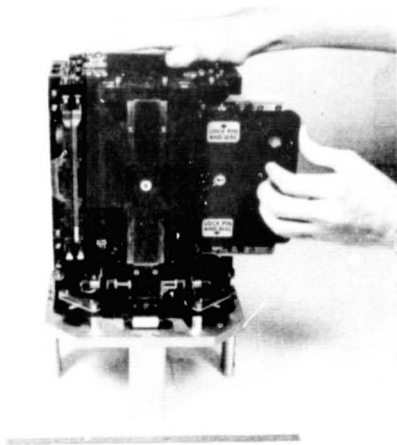


Figure 1. S-149 Micrometeorite collector showing sample cassette loading

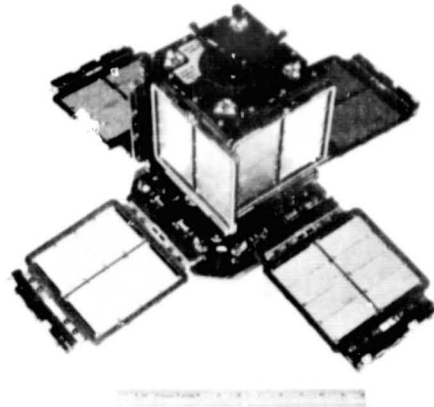


Figure 2. S-149 Micrometeorite collector deployed for exposure

Figure 3 shows the interior of a sample pan loaded with experimental surfaces and foils. All sample pans and covers were photographed in similar fashion before flight and upon return to the Observatory. The overall dimensions of each slide are  $2.9 \times 6.8$  centimeters. Experiments included polished metal slides of stainless steel, copper and silver, sets of  $1\text{cm}^2$  polished slides of copper and stainless steel for scanning electron microscope study, stacked aligned layers of thin ( $400\text{\AA}$ ) carbon-coated nitrocellulose films on electron microscope grids, nitrocellulose films over glass, and 2 layers of  $500 - 800\text{\AA}$  gold foils over stainless steel. In addition, guest experiments were provided by Mr. E. F. Fullam, Dr. H. Fechtig, Dr. J. Geiss, and Dr. W. Krättschmer.

All of the polished metal slides were pre-scanned optically at 200X and the location of any detectable surface irregularities were noted. Furthermore the gold foil samples were pre-scanned by a high resolution photographic technique which mapped all pinholes  $\geq 3\mu$  in diameter. The samples were loaded and unloaded in the Dudley Observatory clean laboratory and stored subsequent to exposure in an argon environment.

Figure 4 shows the location of the S-149 hardware during the antisolar exposure (-Z) through the antisolar airlock, and the location of the hardware during the solar facing exposures (+Z). It is to be noted that the solar facing exposures were manually deployed on the ATM dish by the Sky-

\*Member AIAA

lab crews during their extravehicular activities (EVAs) with the aid of a bracket and crank designed, constructed and qualified at JSC in the short time available between SL/2 and SL/3. This modification was necessary since the Skylab solar airlock had to be used to deploy the sun shield which replaced the spacecraft meteoroid shield.

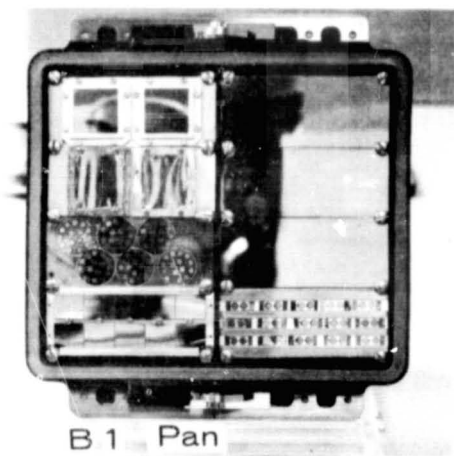


Figure 3. Sample pan loaded for flight

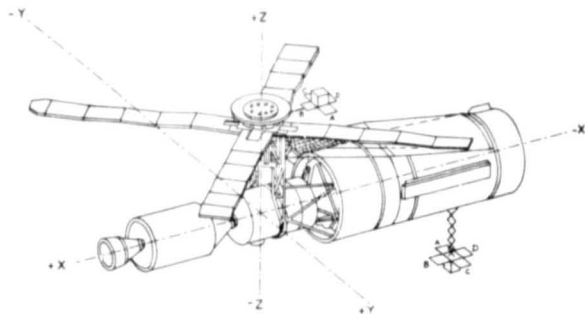


Figure 4. S-149 Exposure locations

Table I shows the beginning and end times of the three exposures carried out and returned to earth thus far. The +Z axis of the spacecraft was maintained toward the sun approximately 99% of the time during these exposures. The angle  $\theta$  between the normal to the A pan ( $\pm Y$ ) and the apex of the earth's motion is also shown together with the average angular deviations during the individual exposure. The exposures were carried out at an altitude of approximately 430 km. The fourth set of cassettes is currently being exposed with the hope that an exposure of multi-year duration can be recovered on a future manned visit to Skylab.

ORIGINAL PAGE IS  
OF POOR QUALITY

Table I Exposure Times

Type	Deployed	Duration	$\theta$
Anti-solar (SL 2/3)	6/23/73	34 days	$149^{\circ} \pm 21^{\circ}$
Solar (SL/3)	8/6/73	46 days	$332^{\circ} \pm 37^{\circ}$
Solar (SL/4)	11/22/73	33 days	$317^{\circ} \pm 18^{\circ}$
Solar (SL/4+)	2/3/74	260 days to date	-

## II. Results

Figures 5 thru 10 show a set of typical hypervelocity impact craters observed in stainless steel and copper slides with a scanning electron microscope. The craters show a raised lip and sidewise compression of the slide material. Figure 5 is one of the largest craters observed and Figure 6 shows an enlarged view of the frozen droplet structure within this crater.

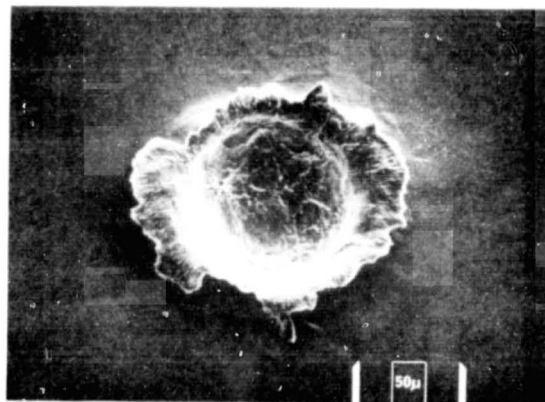


Figure 5. Impact crater in copper

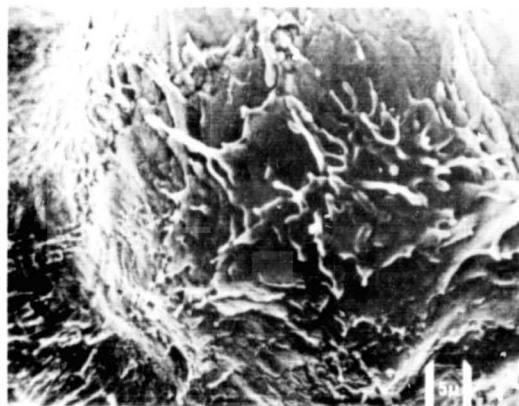


Figure 6. Interior view of crater in Figure 5

Figure 7 shows a small crater within stainless steel which shows a non-symmetric structure, suggestive of the particle impacting at a significant angle with respect to the normal of the polished surface. The crater in Figure 8 was found in an electron microscope grid wire beneath a gold film. The hole in the gold film (approximately  $0.5\mu$  above the grid wire) was enlarged by the blow-out of material from the grid wire during the crater formation. Two such events have been found thus far in the limited area presented by the grid wires under the gold foils.

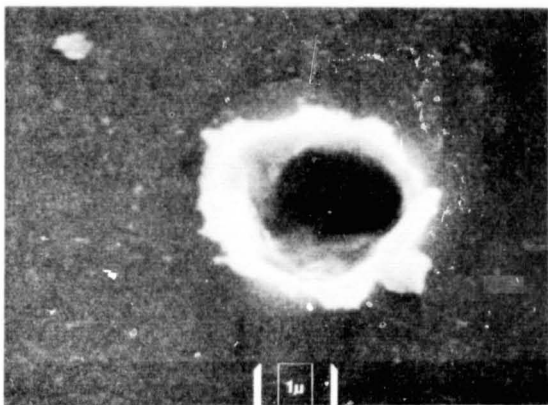


Figure 7. Impact crater in stainless steel

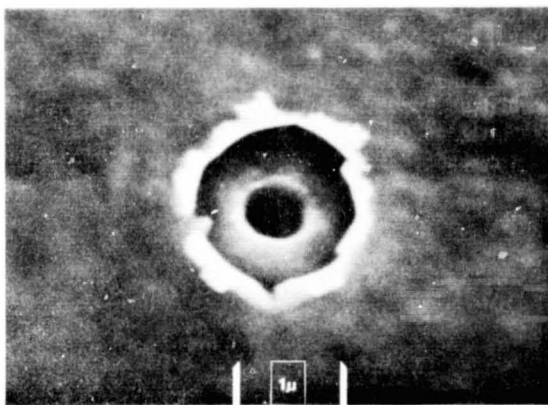


Figure 8. Impact crater in copper grid wire covered with gold foil

Figure 9 shows one of the smallest impact craters observed. This crater was made by a particle  $0.1 - 0.2\mu$  in diameter. The structure of the crater appears to be similar to that of the larger craters. Figure 10 shows two crater events which are close together. A number of such dual events have been noted and appear to be the result of particle breakup near the earth.

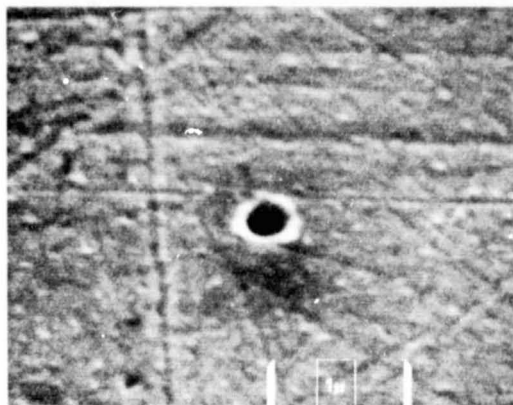


Figure 9. One of the smallest craters found

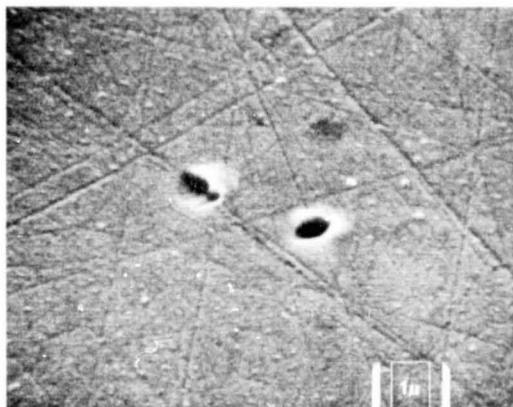


Figure 10. A pair of craters probably resulting from particle breakup

The distribution of the craters in the various pans and covers is shown in Table II. The directions indicated in Table II are the directions perpendicular to the exposed surfaces in the pans and covers with respect to the spacecraft as shown in Figure 4. The data in Table II is an October 1, 1974 summary of the results of optically scanning all metal surfaces once at 200X and some of them at 500X. It will be noticed that the pans have significantly more craters than the covers and that the antisolar covers appear to have more impact craters than the solar facing covers. This is consistent with the concept that the large solid particles of the solar system are spiraling in slowly toward the sun. We anticipate that further work will enable much to be said about the directional characteristics of large micrometeorites.

Table II Crater Locations

Antisolar Airlock (SL 2/3)					
	A	B	C	D	Total
Covers	2 (-Z)	1 (-Z)	1 (-Z)	2 (-Z)	6
Pans	6 (-Y)	5 (+X)	4 (+Y)	2 (-X)	17
Solar Airlock (SL/3)					
	A	B	C	D	Total
Covers	0 (+Z)	0 (+Z)	0 (+Z)	1 (+Z)	1
Pans	7 (+Y)	3 (+X)	3 (-Y)	3 (-X)	16
Solar Airlock (SL/4)					
	A	B	C	D	Total
Covers	0 (+Z)	0 (+Z)	2 (+Z)	1 (+Z)	3
Pans	1 (+Y)	1 (+X)	13 (-Y)	3 (-X)	18

Table III shows a listing of large craters observed from the optical scanning of the large polished metal plates at 200X. It will be noted that the diameter to depth ratio is variable, consistent with the concept that the impacting particles have a range of mass densities and velocities.

Figures 11 through 16 show scanning microscope pictures of four penetration holes in 500 - 800Å thick gold foil. One can see evidence of the non-perpendicular nature of the impact in the asymmetry of the streaks radiating from the penetration hole shown in Figure 11. Figure 12 shows the foil immediately below the penetration hole shown in Figure 11. It will be noted that the penetrating particle broke up into many smaller fragments. This pair of pictures provides a demonstration of the meteoroid shield principle on a miniaturized scale and suggests that some particles are rather fragile, since the dimensions of the particles are very large compared to the thickness of the foil. Some impact craters have been found in the stainless steel substrates beneath the two layers of gold foil. In one case, two small craters 1.5 and 0.5 microns in diameter were found in the substrate after the particle penetrated two layers of gold foil. The hole in the top layer was 25 microns in diameter.

Figure 13 shows the elongated nature of some of the penetration holes, indicative of a near grazing penetration of the cosmic dust particle. Figure 14 shows a penetration hole structure with radial cracks.

Table III 200X Optical Scanning Data

Antisolar Airlock (SL 2/3)			
Cassette Position No.	Surface	Inside Diameter	Inside Diameter/Depth
A Pan	SS	10.4	3.5
A Pan	Cu	7.8	3.0
A Pan	Cu	20.8	1.8
A Pan	Cu	135.2	1.9
A Pan	Cu	19.5	1.9
A Pan	Cu	31.2	1.9
B Pan	Cu	6.9	2.5
B Pan	Cu	3.9	1.8
B Pan	Cu	3.8	2.5
C Pan	Cu	5.4	3.0
C Pan	Cu	5.2	3.3
D Pan	Cu	12.6	3.2
D Pan	Cu	4.0	2.7
B Cover	Cu	6.0	3.0
C Cover	Cu	5.2	5.2
D Cover	SS	6.5	2.4
D Cover	Cu	14.3	2.3
Solar Airlock (SL/3)			
Cassette Position No.	Surface	Inside Diameter	Inside Diameter/Depth
A Pan	Cu	6.5	3.3
A Pan	Cu	5.8	1.9
A Pan	Cu	5.8	2.3
B Pan	SS	6.5	2.2
B Pan	Cu	46.8	2.1
C Pan	Cu	4.5	2.3
C Pan	Cu	3.9	2.8
C Pan	Cu	3.9	2.2
D Pan	Cu	18.2	1.9
D Pan	Cu	4.3	2.9
D Pan	SS	4.4	3.1
D Cover	Cu	5.8	1.9
Solar Airlock (SL/4)			
Cassette Position No.	Surface	Inside Diameter	Inside Diameter/Depth
A Pan	Cu	3.4	3.4
C Pan	Cu	5.2	5.2
C Pan	Cu	3.9	3.9
C Pan	Cu	2.6	2.6
C Pan	Cu	2.6	2.6
C Pan	Cu	2.5	2.5
C Pan	Cu	6.5	3.3
C Pan	Cu	3.7	3.7
C Pan	Cu	4.6	3.2
D Pan	SS	20.8	2.3
C Cover	SS	7.8	5.2
C Cover	SS	8.0	2.7
D Cover	Cu	6.5	3.3

ORIGINAL PAGE IS  
OF POOR QUALITY



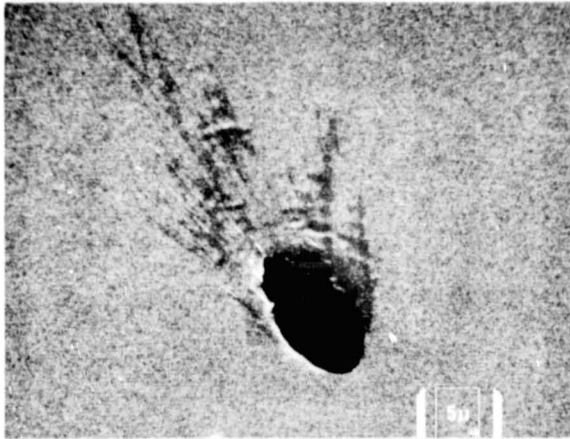


Figure 11. Penetration hole in gold foil

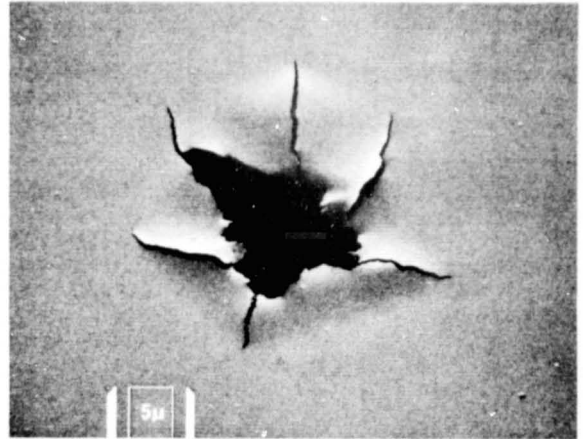


Figure 14. Penetration hole with radial cracks

Figures 15 and 16 indicate that occasionally some of the impacting particle remains in the vicinity of the hole structure. Figure 16 also has several penetration holes close together suggesting that the particle broke up before penetrating the gold foil.

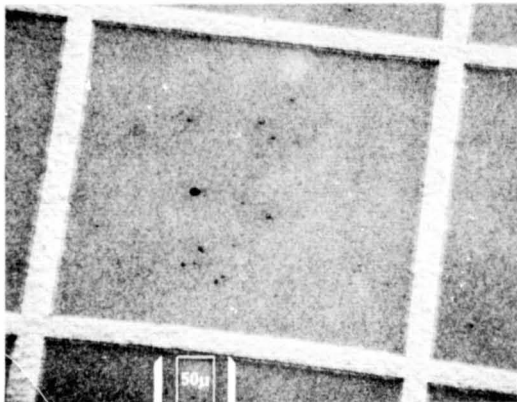


Figure 12. Multiple holes made by fragments of the same particle which produced the hole in Figure 11

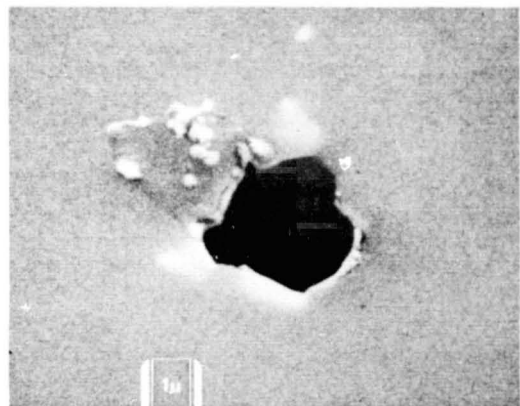


Figure 15. Penetration hole with debris from impacting particle



Figure 13. Elongated hole in gold foil

Figure 17 shows a photograph of three exposed silver slides compared with an unexposed control silver slide. It will be noticed that a thick black corrosion layer developed on the silver slides during the solar exposures and a thinner layer resembling tarnish developed during the anti-solar exposure. X-ray diffraction analysis has shown the black material on the silver to be silver oxide ( $\text{Ag}_2\text{O}$ ). The copper slides showed a smaller but noticeable amount of oxidation. The  $\text{Ag}_2\text{O}$  layer on the solar facing sample was approximately  $2\mu$  thick. This oxidation layer on the silver sample was sufficiently thick that these samples were not used for crater counts.

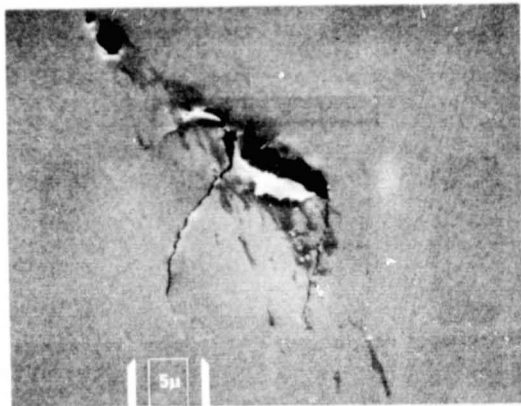


Figure 16. Penetration hole resulting from a particle which had broken up before impacting

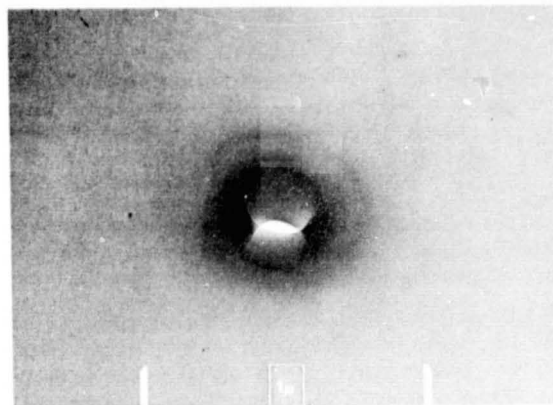


Figure 18. "Evil eye" structure

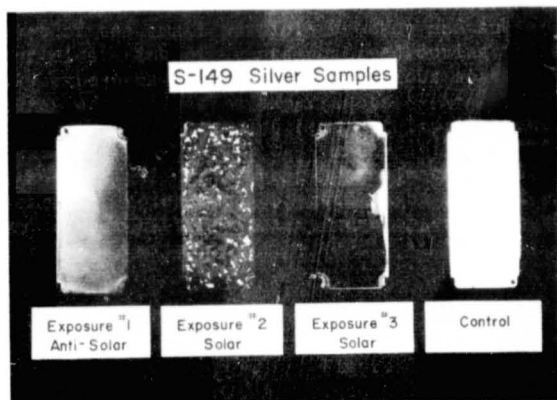


Figure 17. Silver samples

The oxidation is the result of chemical reaction with atomic oxygen in the ionosphere. Such an oxidation mechanism appears to explain at least a part of the small particle breakup and subsequent clustering of events observed during these S-149 exposures as well as on previous space exposures and collection experiments.<sup>(1)(2)</sup> One of the best examples of clustering of impact events due to particle breakup was observed in an anti-solar cover gold foil where approximately 1000 penetration holes were observed in an area of only  $8 \text{ mm}^2$ . Most of the clusters were observed on the solar facing exposures.

Figure 18 shows an "evil eye" structure of a type similar to that observed during the S-12 exposure during Gemini 9.<sup>(1)</sup> Figure 19 shows the same "evil eye" with the nitrocellulose film tilted about  $20^\circ$  to reveal more clearly the cylindrical nature of the hole. We believe we can gain significant directional data from the "evil eyes" in future studies. It appears that particles making the "evil eye" structure are the same as the high density core particles observed in our rocket collection program.<sup>(2)</sup>

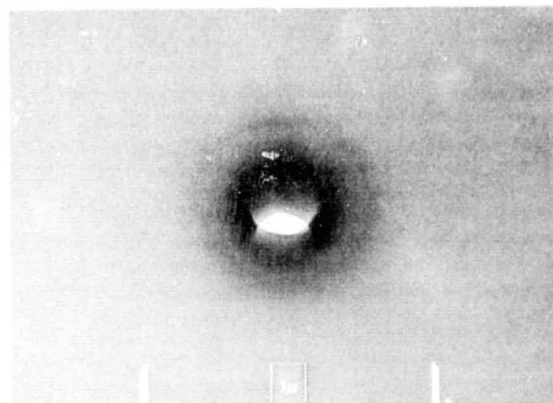


Figure 19. "Evil eye" structure rotated  $20^\circ$

Figure 20 shows the flux curve from the data analyzed thus far. It will be noticed that in the large particle size range ( $10^{-12}$  -  $10^{-7}$  grams) the data is consistent with the S-10 data from Gemini 8 - 10,<sup>(1)</sup> and somewhat higher than the Explorer data.<sup>(3)</sup> The fluxes obtained with the crater data appear to be significantly higher in the antisolar exposure than in the solar exposure suggesting that these large particles are spiraling inward toward the sun. These crater fluxes have been plotted using combined pan and cover data. Table II shows that the number of crater events in the pans was significantly greater than the number in the covers. Thus the fluxes of large particles in the plane perpendicular to the direction to the sun would be much greater than the fluxes of large particles in the solar and antisolar directions.

The "evil eye" fluxes observed during the solar exposures appear to be within the range of fluxes of submicron particles observed in the rocket collection experiment<sup>(2)</sup> and are consistent with the fluxes given by the "evil eyes" on the S-12 experiment of Gemini 9.<sup>(1)</sup>

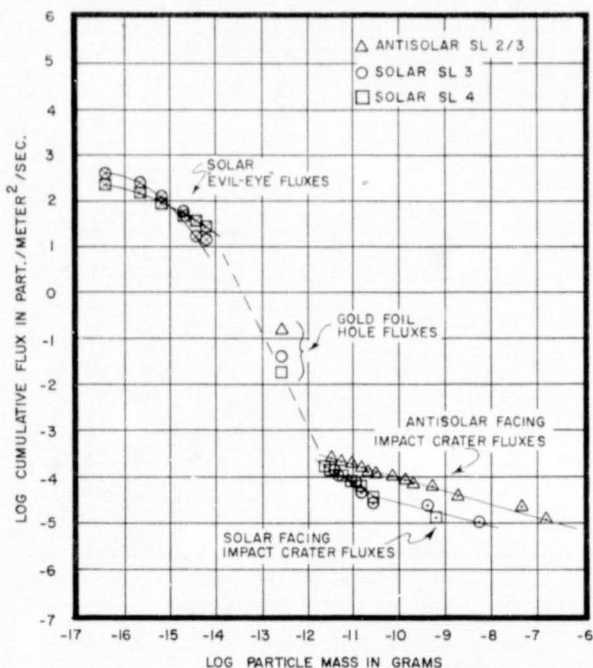


FIGURE 20 S-149 PARTICLE FLUXES

The crater sizes have been converted to particle masses by assuming that the particle densities are  $3 \text{ gm/cm}^3$  and that the particle diameters are one third the crater inside diameters. The "evil eye" fluxes and the gold foil fluxes were computed by assuming a density of  $3 \text{ gm/cm}^3$  and a ratio of hole diameter to particle diameter of two. The fluxes have been corrected for solid angle of view and earth shielding.

Interesting data has also been obtained by the guest experimenters on S-149:

1) Dr. Fechtig<sup>(4)</sup> from the Max Planck Institut für Kernphysik at Heidelberg reported at COSPAR (1974) the finding of a cluster of 40 small impact craters in  $4 \text{ cm}^2$  of a pyroxene sample exposed in the solar facing direction.

2) Dr. Krättschmer also of Max Planck Institut für Kernphysik at Heidelberg exposed some phosphate glass slides to study low energy, high Z cosmic ray tracks and will report his interesting findings elsewhere when his studies are complete.

3) One of the most exciting results from S-149 has been obtained by Mr. E. F. Fullam, who exposed Lexan slides in the solar and antisolar directions and appears to have found fission track clusters indicating the presence of uranium or thorium in the solar facing samples but not on the antisolar facing samples. This result, if confirmed by further study provides additional evidence of high temperature refractory elements in particles emitted by our sun.<sup>(5)</sup>

4) Dr. J. Geiss from Switzerland exposed a few slides in S-149 to serve as supplemental exposures to his S-230 exposures. He is saving the S-149 exposures until he has completed more of his S-230 analysis.

The cosmic dust data from S-149 supports the concept of the solar system containing two populations of particles, a submicron component flowing outward from the sun<sup>(2)(5)(6)</sup> and a larger group of particles slowly spiraling inward toward the sun. Furthermore the S-149 experiment has provided clear evidence of particle breakup near the earth and an oxidation mechanism for this particle fragmentation has been suggested.

Much more work remains to be done and the full study and calibration of the S-149 materials will take many years and shows promise of determining accurately the near-earth population of cosmic dust particles over a wide mass range.

We wish to express our appreciation to the flight crews and flight controllers of SKYLAB for their competent and enthusiastic assistance, to Mr. William Schneider, Mr. Kenneth Kleinknecht and Mr. Mitch Willcox and their associates for their extraordinary support and encouragement in carrying out this experiment. We also thank L. Bourdillon, C. Jones, A. Laudate, B. Reynolds, J. Tarnawski, L. Brennan, P. Hutchison, W. Radigan and R. Schwarz of the Dudley staff for the design, qualification of the instrument, the sample preparation and the many hours of painstaking scanning. This work was carried out under NASA Contract NAS9-10380.

#### References

1. Hemenway, C. L., Hallgren, D. S. and Kerridge, J. F., "Results from the Gemini S-10 and S-12 micrometeorite experiments," Space Research VIII, 510, Amsterdam, North Holland, 1968.
2. Hemenway, C. L., invited paper presented at the Symposium honoring F. Whipple, Smithsonian Contribution to Astrophysics, Cambridge, 1973, in press.
3. D'Aiutolo, C. T., Kinard, W. H., and Naumann, R. J., "Recent NASA meteoroid penetration results from satellites," in Hawkins, Gerald S., ed., Meteor Orbits and Dust: The Proceedings of a Symposium, Cambridge, Mass., 1965. Smithsonian Contributions to Astrophysics, v. 11. Washington, NASA, 1967 (NASA SP-135), p. 239.
4. Nagel, K., Fechtig, H., Schneider, E., and Neukum, G., "Micrometeorite impact craters on Skylab experiment S-149," COSPAR, 1974, Sao Paulo, Brazil.
5. Hemenway, C.L., Hallgren, D.S. and Schmalberger, D.C., "Stardust," Nature, v.238, 256,1972.
6. Hemenway, C.L., Erkes, J.W., Greenberg, J.M., Hallgren, D.S. and Schmalberger, D.C., "Do some of the sub-micron cosmic dust particles come from the sun?" Space Research XIII, 1973.

ORIGINAL PAGE IS  
OF POOR QUALITY

## APPENDIX D

### MICROMETEORITE PENETRATION EFFECTS IN GOLD FOIL

Douglas S. Hallgren, Dudley Observatory, Albany,  
New York, U. S. A.

Curtis L. Hemenway, Dudley Observatory and the  
State University of New York at Albany, Albany,  
New York, U. S. A.

William Radigan, Dudley Observatory and the  
State University of New York at Albany, Albany,  
New York, U. S. A.

Single and double layers of 500 - 800 Å thick gold foil exposed on the S-149 Skylab experiment have revealed a variety of penetration structures. A wide range of particle strength is evidenced by the degree of break-up the particle apparently experiences upon interaction with the first layer of gold foil. Even particles which must be large compared to the foil thickness often are shattered upon penetrating the foil. The foils have detected clusters of particles containing from a few to several hundred particles. The extreme fragility of some particles is shown by the case of one particle which broke into several thousand particles a few centimeters above the foil. Because of the extreme morphological variety in penetration effects a precise relationship between the size of the event and the mass of the particle producing it has not been determined but probably has a mass of  $10^{-13}$  gm and shows a flux value of  $8 \times 10^{-3}/\text{m}^2 \text{ sec}$ .

(Preprint of Paper III. C.4 presented at COSPAR meeting at Varna, Bulgaria)

(June 1975)

## INTRODUCTION

One part of the S-149 experiment on Skylab<sup>1</sup> was designed to detect holes made by micrometeorites in thin unbacked gold foils. The intent was to provide data about the micrometeorite flux in the mass range of  $10^{-12}$  to  $10^{-9}$  grams. The gold foils were 500-800Å thick, supported by 90 mesh copper screening, and were exposed in sets consisting of a single and a double layer mounted above a polished stainless steel plate. The foils were located such that they were exposed in all possible directions. Figure 1 shows the deployment of the S-149 experiment in the +Z (solar) and -Z (anti-solar) directions.

Since it is nearly impossible to produce thin foils that are pinhole-free it was necessary to record the condition of each foil before the flight. This was accomplished by using each foil as a negative and printing an image on the foil on enlarging paper. In this way all holes greater than 3 microns existing before the flight could be noted by visual examination of the print. It was later found that, in many cases, holes as small as one micron could be detected on the pre-flight photograph. The best control for this experiment, however, turned out to be those portions of the double layer films on which the number of impact events was low. These foils had experienced the full thermal, vibrational, and shock environment of the mission but no small holes were found induced in them owing to this history of stress.

Figure 2 shows a type of hole which we have labeled an event of Type I. Events of this type were found randomly oriented on the C and D

cassettes and are believed to be genuine cosmic dust events but a large number, with common orientations, found on cassettes A and B from S/L 3 have been identified as the result of secondary ejecta from a collision of a micrometeorite with the ATM. The elongation of the hole and pile-up of debris on the trailing edge of the holes makes it possible to determine the direction from which the particles came. Confirmation of this interpretation is found in the chemical analysis of the residues around the Type I events in the A and B cassettes. These are found to contain a significant quantity of aluminum. The 141 events of Type I were distributed as shown in Table 1.

The foils have recorded other events and each contains information pertinent to the nature of micrometeorites but not all of them are fully understood.

The second type of penetration hole identified as a valid event has been termed an event of Type II. These events characterized by Figures 3 and 4 have the widest distribution over all the cassettes (see Table 1) and appear as jagged holes occasionally showing a small build-up of material on the edges. Locally high concentration of these events were found on cassette B from S/L 3 and on cassette C from S/L 4. This suggests a marked spatial inhomogeneity of the incoming particles. Some of the Type II events on cassette B have also been identified as artifacts. These events were produced by secondary ejecta containing paint particles from the ATM. This paint contains ZnO in a silicone matrix, and both Zn and Si

Table 1

Distribution of Foil Events

Flight	S/L 2-3 <sup>1</sup>				S/L 3 <sup>2</sup>				S/L 4 <sup>2</sup>			
Date Deployed	June 23, 1973				August 6, 1973				Nov. 22, 1973			
Duration	34 days				46 days				33 days			
Type of Event	I	II	III	IV	I	II	III	IV	I	II	III	IV
Cassette												
A Pan Cover	0	2	1	1	75 <sup>3</sup>	2	1	0	0	9	0	1
	0	0	0	0	43 <sup>3</sup>	0	0	0	7	2	0	0
B Pan Cover	5	1	0	0	13 <sup>3</sup>	97 <sup>4</sup>	6	3	0	10	1	1
	0	0	0	0	1 <sup>3</sup>	10	2	3	0	3	0	1
C Pan Cover	0	4	1	0	0	1	0	0	0	0	3	0
	0	0	0	0	0	9	1	1	1	310 <sup>4</sup>	14 <sup>4</sup>	18 <sup>4</sup>
D Pan Cover	0	4	0	0	0	0	0	0	1	3	1	2
	0	5000	0	0	0	1	0	0	0	1	0	0

1 Anti-solar facing

2 Solar Facing

3 Secondary events - not counted in flux

4 Cluster events - not counted in flux



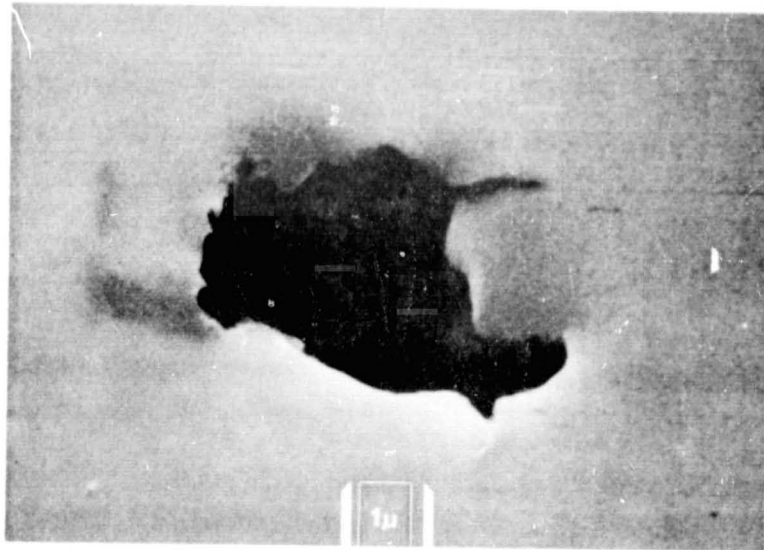


Figure 3  
Type II Event in Gold Foil

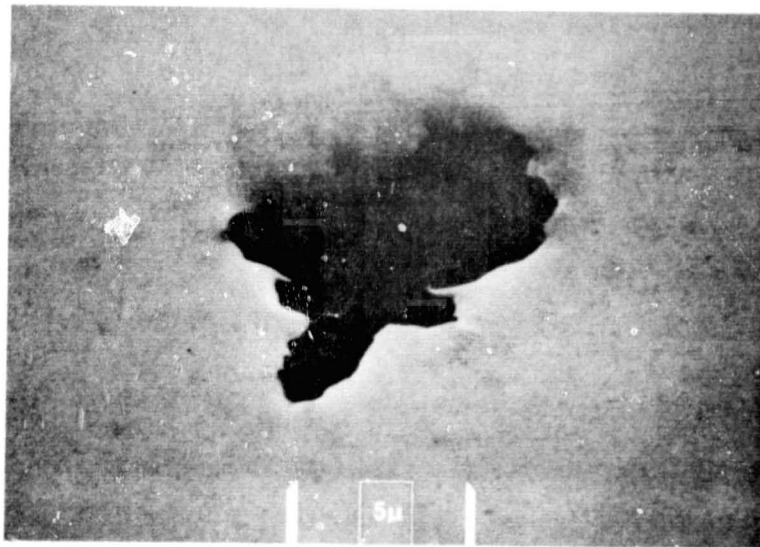


Figure 4  
Type II Event in Gold Foil

**ORIGINAL PAGE IS  
OF POOR QUALITY**

16-2B

have been clearly identified in the debris around some of the holes.

Two other valid types of penetration events are illustrated in Figures 5 and 6. Events of Type III (see Figure 5) show generally symmetric holes with radial cracks. Events of Type IV (see Figure 6) are elongated and often have a portion of the foil folded back on itself.

The most unusual event occurred on a foil in the cover of the D cassette exposed during S/L 2-3. An estimated 5000 holes in the size range of 1-3 microns were found in an area of about  $8\text{mm}^2$ . Measurement of the orientation and shape of the holes indicated that the original particle must have been 1-2 cm above the foil when it broke-up. Figure 7 shows the reconstructed event schematically. Based on a density of  $3\text{gm/cm}^2$  the original particle has a mass of  $1.5 \times 10^{-8}$  gm and a diameter of 15 microns.

#### DISCUSSION

Systematic examination of all double layered gold foils showed that particles producing holes (of any type) greater than five microns in diameter in the first foil break up into many fragments which in turn produce many more holes in the second foil. Typically the hole pattern in the second layer consists of 3-5 holes 1-2 microns in diameter plus 20-100 or more holes with diameters as small as 0.1 micron. It is interesting to note that particles that produce events of Type 1 in the first foil also produce Type I events in the second foil. Figure 8 shows a portion of a typical distribution of holes in a second layer.

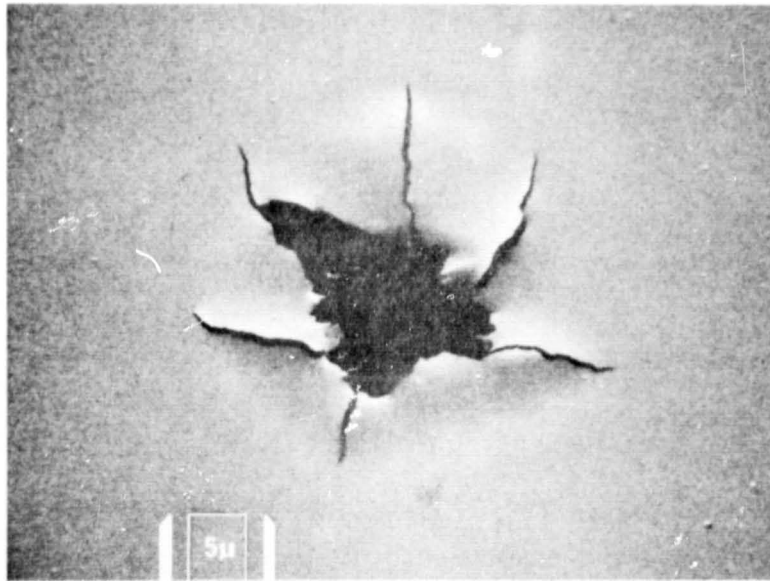


Figure 5  
Type III Event in Gold Foil

ORIGINAL PAGE IS  
OF POOR QUALITY



Figure 6  
Type IV Event in Gold Foil

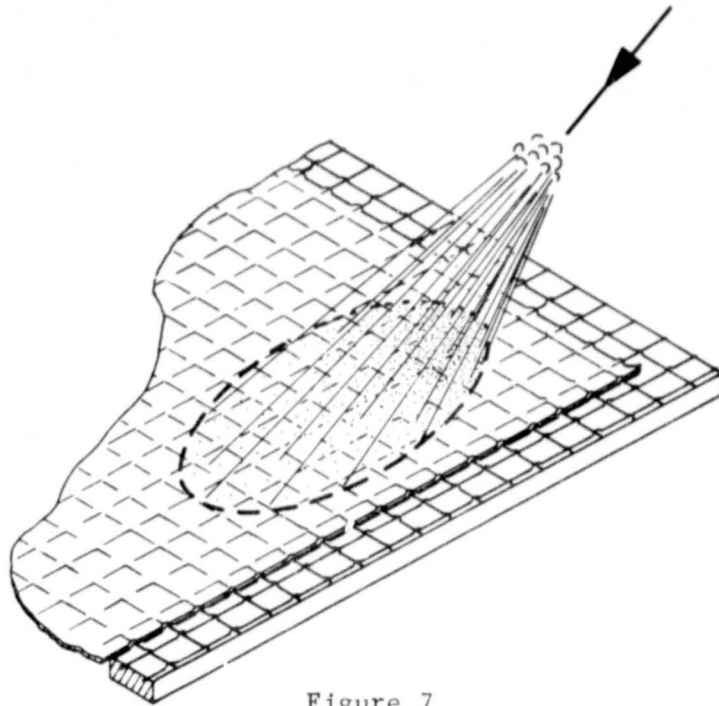


Figure 7  
Conceptual Drawing of the Break-up  
of a Particle Before Striking Gold Foil

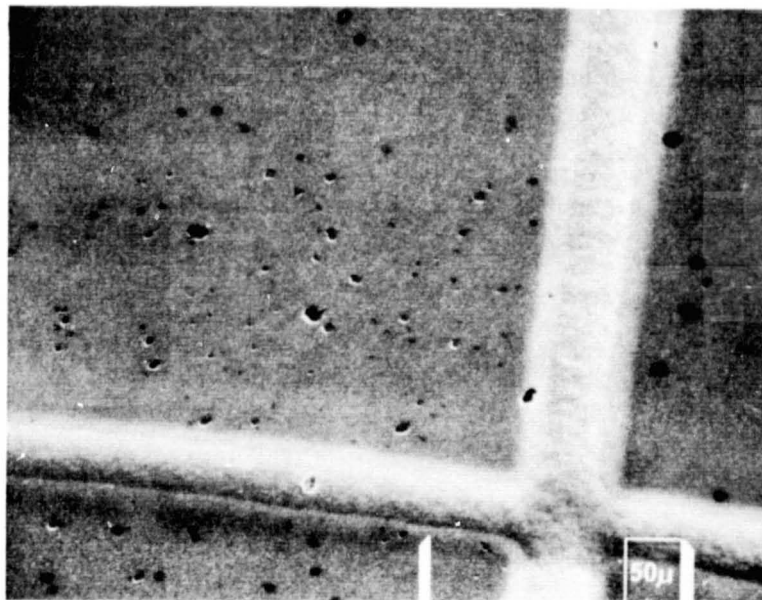


Figure 8  
Holes in the Second Layer of Gold Foil

No evidence of an original particle was found on any stainless steel plate, below the foils, with but one exception. In the later instance the particle made a 25 x 65 micron hole in the top foil, a hole greater than 100 microns plus smaller holes in the second foil and, finally, a 2 micron crater in the stainless steel.

In this connection, we have looked carefully at events produced in test firings on single layer gold foils using the accelerator at the Max-Planck-Institut at Heidelberg. Iron particles with about 1.2 micron diameter average size traveling at velocities at 5-6 Km/sec produced holes which averaged 2 times the particle diameter.

In these calibration experiments the particle diameter to foil thickness ratio is about 20, the edges of the holes produced are smooth, and craters are always found in the underlying stainless steel plates; i.e. the particle survives the foil impact intact to produce a crater. Now, other studies have shown <sup>2,3</sup> that when the diameter of an impacting particle is of the order of the thickness of the foil it will shatter upon impact. Assuming that the same ratio of hole to particle diameter occurs in Skylab as is found in the calibration experiments then those particles making holes greater than about 5 microns in diameter in Skylab foils must have a diameter greater than about 2.5 microns. These particles then, will have a diameter to foil thickness ratio of 30 or more and so should produce a smooth hole with an underlying crater. The fact that, instead, such particles shatter completely on impact suggests that they are either of a

fluffy nature or are very loose aggregates.

In computing a flux from the gold foil data those events produced by the cluster impacts have been omitted. A density of  $1\text{gm/cm}^3$  and a hole to particle diameter ratio of 2 have been assumed. In addition the data has been corrected for earth shielding and field of view on the spacecraft. Table 2 shows the combined effect of the various correction factors.

Table 2  
Combined Shielding Factors (%)

Cassette Half	Solar	Anti-solar
Cover	52.8	56.3
Pan	40.9	43.6

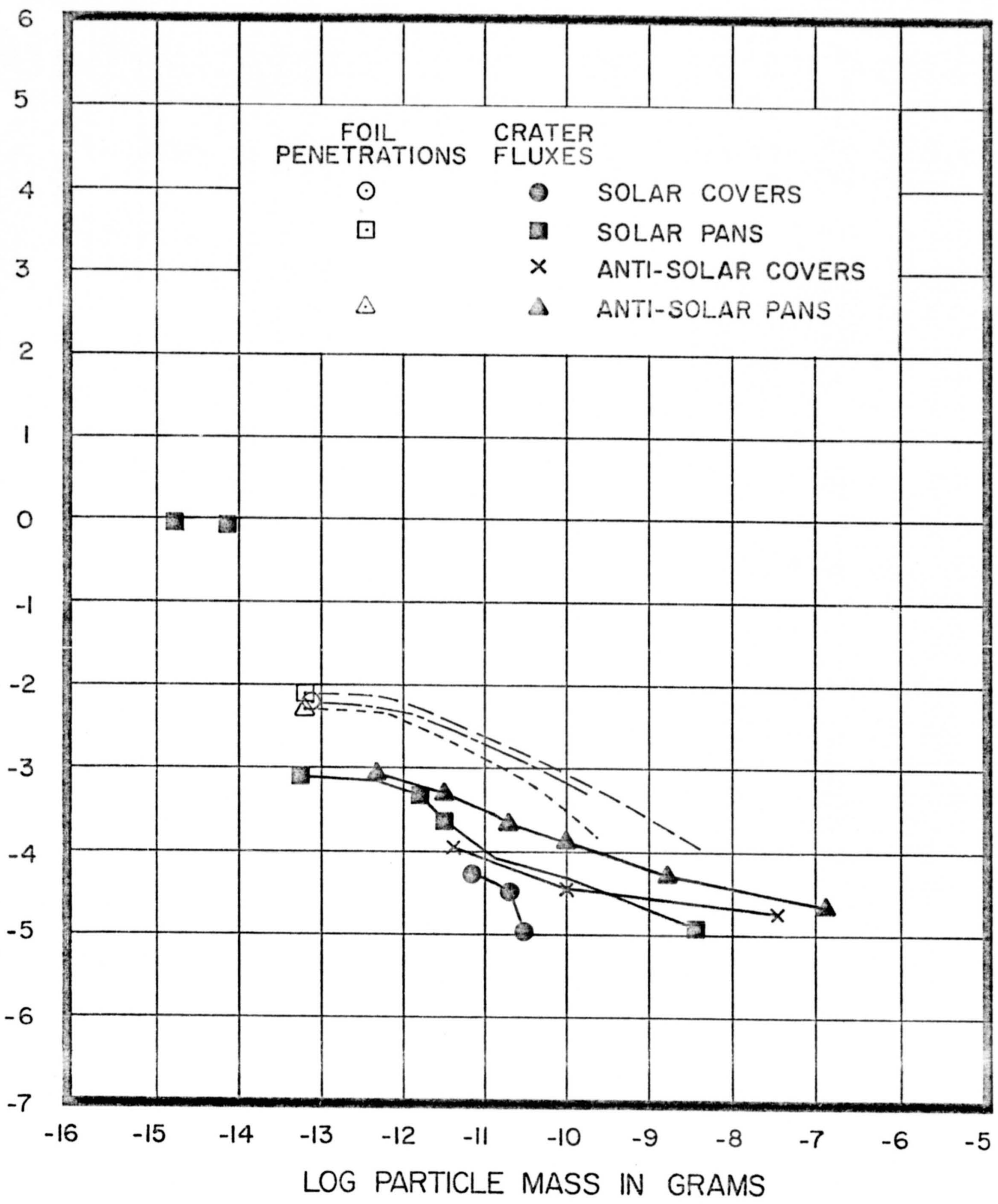
Figure 9 shows the flux curve. The mass points shown are based on the limited calibration data available. If we assume that the same particle to hole relationship exists for larger holes then the flux curve for the gold foil data appears as shown by the dashed lines. Over the range of mass observed the flux appears to be one order of magnitude greater than that computed from the results of crater impact studies. If one assumes that the number of clusters observed represent a steady state condition and the results of these events are then added to the flux curve by considering each hole as a separate event then the curve would rise by about a factor of 5 at the low mass end and the slope would become steeper.

In the study of impact craters (CON 9-149<sup>4</sup>) it was noted that virtually all of the craters were found on the pans suggesting predominately heliocentric elliptic orbits. We note that the foil fluxes are essentially the same on the solar and anti-solar facing pans and on the solar facing covers; however the anti-solar facing covers recorded no influx of foil events. A comparison of the crater and foil fluxes would seem to imply that the foil events resulted from fragile particles of low bulk density in a hyperbolic orbit moving outward from the direction of the sun.

The size of the events studied to date has been limited to one micron diameter by the effective resolution limit of the light optical system. Further studies using electron optical techniques should reveal the effects of particles as small as 0.1 micron in diameter.

The authors wish to express their appreciation to A. Laudate and R. Schwarz in gathering the data and preparation of the foils for the experiment. This work was supported by NASA Contract NAS 9-10380.

LOG CUMULATIVE FLUX IN PART./METER<sup>2</sup>/SEC.



16-6a



References

1. C. L. Hemenway, D. S. Hallgren and C. D. Tackett, "Near Earth Cosmic Dust Fluxes from S-149", AIAA/AGU Conference on Scientific Experiments of Skylab, Huntsville, Alabama, 1974.
2. S. Auer, E. Green, P. Rauser, V. Rudolph and K. Sitte, "Studies on Simulated Micrometeoroid Impact", Space Research VIII, North Holland Amsterdam, 1968, p. 606.
3. A. R. Lewis and R. A. Walter, "The Film Penetration by Hypervelocity Microparticles", NASA-TM-X-2065, Washington, 1971.
4. C. L. Hemenway, D. S. Hallgren and A. T. Laudate, "Analysis of Impact Craters from the S-149 Skylab Experiment", IAU Colloquium 31, Heidelberg, 1975.

## APPENDIX E

### ANALYSIS OF IMPACT CRATERS FROM THE S-149 SKYLAB EXPERIMENT

D. S. Hallgren and C. L. Hemenway  
Dudley Observatory and State University of New York at Albany,  
Albany, N. Y. USA

#### Abstract

Analysis of craters found on polished plates exposed during Skylab has provided data for a flux measurement over the mass range  $10^{-15}$  to  $10^{-7}$ gms. Chemical analysis of residues in the craters shows a high incidence of aluminum. A variety of morphological forms are described.

A major part of the S-149 experiment<sup>1</sup> on Skylab involved the study of impact craters on highly polished metal surfaces. Samples of polished copper, stainless steel, and silver were exposed in sets of four cassettes, each set having a polished plate sample area of  $0.06\text{m}^2$ . Each cassette is in two parts, a stationary half called the "pan" and a movable half called the "cover". During exposure the covers face in either the solar or anti-solar direction. Figure 1 illustrates the deployment of the S-149 experiment in the solar and anti-solar modes. The Z axis direction was highly stabilized with respect to the sun but the spacecraft underwent slow oscillation about Z. The pans, therefore, being parallel to the Z axis were not directed toward a fixed direction in space. Table 1 shows the exposure data for each of the three sets of cassettes which were returned. A fourth set of samples is currently being exposed awaiting a possible future return to Skylab.

Optical scanning is the principal method used for the detection of craters. All of the samples have been scanned at 200X, and about 25% have been re-examined at 500X. In addition a small area (approx.  $63\text{mm}^2$ ) has been scanned in a scanning electron microscope at 5000X. The optical scanning to date has revealed a total of 78 craters ranging in size from  $1.9\mu$  inside diameter to  $135\mu$  inside diameter. The small area studies in scanning microscope have shown six classic submicron craters as small as  $0.3\mu$ . The

fluxes computed from the data are shown in Figure 2.

<u>Type</u>	<u>Deployed</u>	<u>Duration</u>
Anti-solar (SL 2/3)	6/23/73	34 days
Solar (SL/3)	8/6/73	46 days
Solar (SL/4)	11/22/73	33 days

Table 1  
Exposure Times

Due to the orientation of the collector, the region of space seen by the pans is the same for both the solar and anti-solar exposures while the covers point along a single axis. In each case the fluxes for the pans exceed those for the covers by a factor of 5 to 10. Note in Figure 2 that the fluxes computed from the submicron craters found in the scanning electron microscope are higher than those for the larger craters by a factor of about  $10^3$ .

All fluxes were computed using a crater-to-projectile diameter ratio of 3 which presumes all particles to have the same densities and impacting velocity. Shielding factors to correct for the field of view for each pan and cover were applied in the flux calculation; these are listed in Table 2.

Cassette Half	Solar	Anti-solar
Cover	52.8	56.3
Pan	40.9	43.6

Table 2  
Combined Shielding Factors (%)

In addition to the flux determination the craters have been examined in the scanning electron microscope to study the variability in morphology of the crater interiors. This data has been compared with chemical analyses of the residues seen in the crater interior.

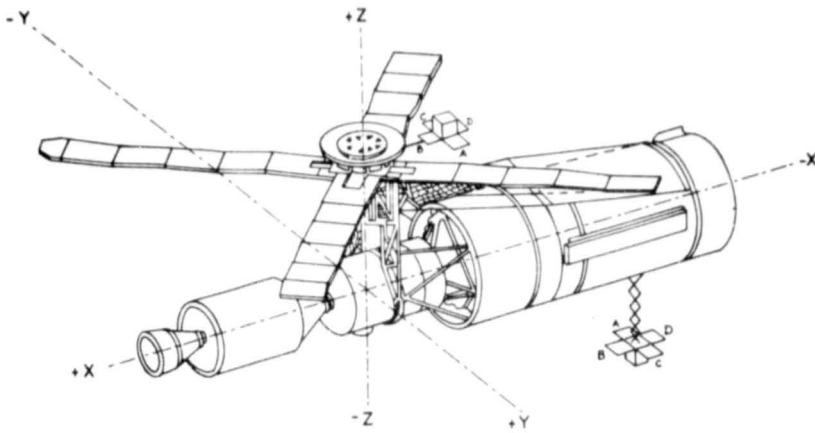


Figure 1  
Schematic of S-149 Deployment

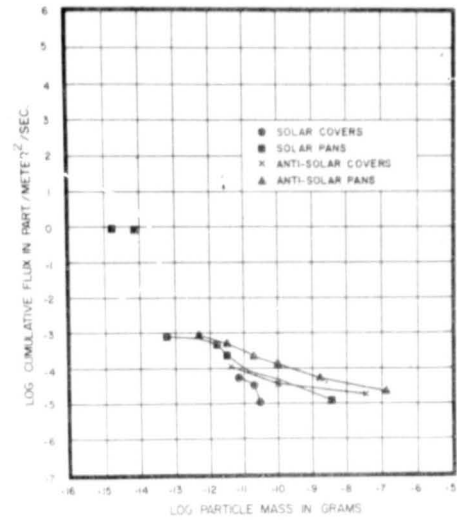


Figure 2  
Flux Curve From Crater Data

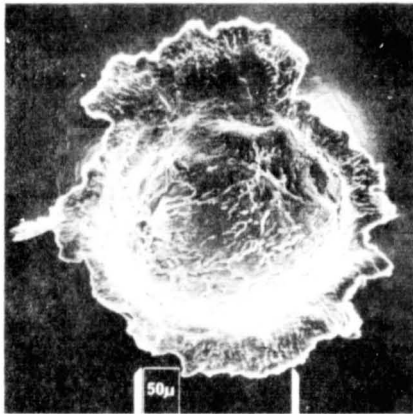


Figure 3  
Impact Crater with Melted Interior

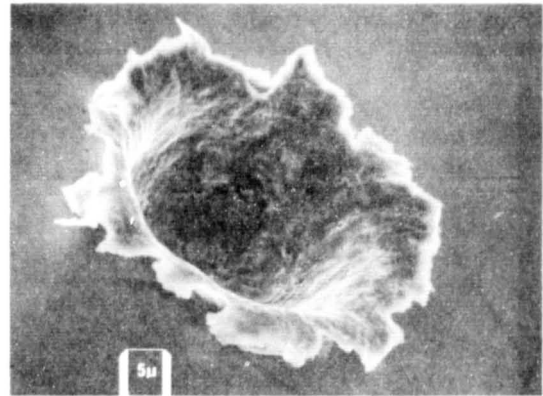


Figure 4  
Impact Crater with Textured Interior

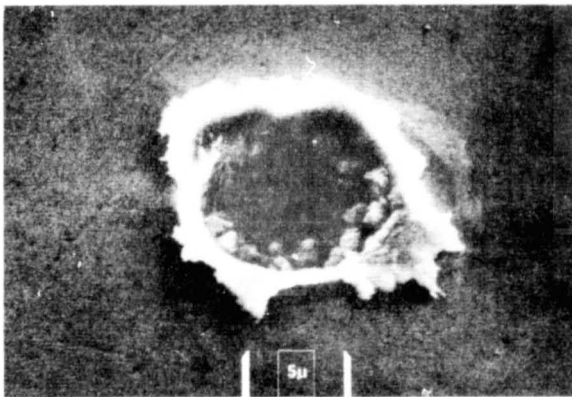


Figure 5  
Impact Crater with Lumpy Interior

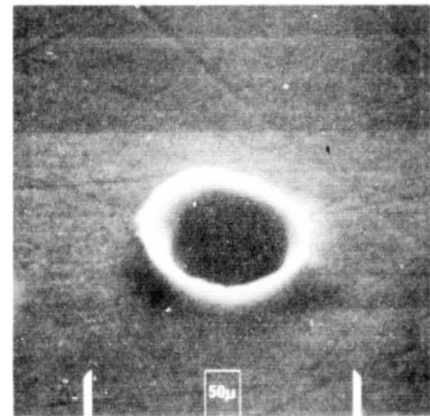


Figure 6  
Impact Crater with Smooth Interior

Figures 3 - 6 show representative examples of four general types of crater morphology observed on copper plates. In Figure 3 the crater interior shows distinct signs of melting. This type of structure was limited to the larger craters i.e. greater than  $20\mu$  inside diameter.

Figure 4 shows an example of the most prevalent structure. The term "textured" has been used to describe the generally rough interior.

Figure 5 shows one of three craters in which lumps of residue could be seen within the crater. The last type, shown in Figure 6, has no internal structural detail.

While it is apparent that the craters in Figure 5 and 6 show distinctly different interior structure we emphasize that the structures seen in Figures 3 and 4 are also sufficiently distinct to define crater types. Because of what looks like a sequence of potential physical relevance in these micrographs, attempts were made to correlate morphology with observed parameters such as crater diameter, crater depth and diameter to depth ratio; no systematic relationship could be established. It would appear that crater morphology may be related to other physical parameters involved in the collision such as the strength and structure of the original particle.

Chemical analysis of the interior walls and lips of the craters was carried out using an energy dispersive x-ray spectrometer in the scanning electron microscope for counting times of 100 - 1000 seconds. Even though there appear to be distinct types of craters as seen from the morphology no classification can be made on the basis of the residual elements from the impacting particle detected within the craters. Size alone does not determine the ability to detect residues: some craters one micron or less in diameter show residues while the largest crater analyzed showed no detectable residue

even with long counting times (1000 sec.). As seen in Table 3, the element most frequently detected was aluminum and, in all, 10 different elements have been detected. Residues may be found exclusively on the lips of a crater, exclusively in the interior, or distributed over either but it is not possible to predict from the appearance of a crater alone where the residue will be found. About 55% of the impact craters yielded detectable residual elements.

Type	Dia ( $\mu$ )	Dia/depth	Elements						
<u>Smooth</u>									
B-1-12-2	5.2	4.3	Al						
C-2-9-9-2	1.8					Cr	Fe	Ni	
<u>Melted</u>									
B-1-12-1	47	2.1						Fe	
A-3-15-2	21	1.8	Al						
A-3-16-2	20	1.9	Al						
A-3-16-3	31	1.9	Al						
<u>Lumpy</u>									
B-1-12-4	15	3.9	Mg	Al	Si	S	K	Fe	Ca
B-2-9-3-1	1.8	-			Si	S	Zn		
B-3-15-9-1	12	2.6		Al					
<u>Textured</u>									
B-1-12-3	7.8	2.8	Mg		Si				
D-2-16-8-1	2.5	-		Al	Si				
A-3-15-1	7.8	3.0		Al					
B-3-13-1	6.9	2.5			Si	S		Fe	
C-3-14-1	5.6	3.1		Al					
C-3-14-2	5.4	3.6		Al					
C-3-14-4	4.9	4.1		Al					
C-3-14-5	6.5	3.3		Al					
C-3-16-1	2.1	-		Al	Si				

Table 3  
Elements Detected Within Craters

It might be supposed that detection of many craters with aluminum residues indicates that the craters were produced by secondary impacts resulting from micro-meteorites striking the spacecraft. There is a possibility of this happening during

the solar exposure<sup>2</sup> but on the anti-solar exposure, where most of the aluminum containing craters were found, this is highly unlikely because the S-149 samples were out of the field of view of most of the spacecraft.

In summary the S-149 experiment has provided a long duration measurement of the micrometeorite flux in near-earth vicinity over the mass range  $10^{-15}$  to  $10^{-7}$  gm. Over this mass range the flux is observed to be greater by about an order of magnitude than those measured on the lunar surface. A sharp discontinuity is suggested in the flux at a mass of about  $10^{-13}$  gm. The fact that 70 out of the 78 craters found were on the pans indicates that most of the detected particles were in near circular helio-centric orbits. Examination of the crater interiors as seen in the scanning electron microscope indicates that there are considerable variations in the interior structures of the micrometeorite impact craters. Detection of residual elements from micrometeorites within the craters has been successful for craters even those as small as one micron. The most frequently detected element is aluminum which, considering meteoritic abundances, is quite surprising. Evidence for particle clustering has also been found.

This work was supported by NASA contract NAS9-10380 and NAS8-31516.

#### References

1. C. L. Hemenway, D. S. Hallgren and C. D. Tackett, "Near-Earth Cosmic Dust Results from S-149", AIAA/AGU Conference on Scientific Experiments of Skylab, Huntsville, Alabama, 1974, AIAA Paper 74-1226, p. 7.
2. D. S. Hallgren, C. L. Hemenway and W. Radigan, "Micrometeorite Penetration Effects in Gold Foil", COSPAR, Varna, Bulgaria, 1975, Space Research XVI, in press.